

Online Appendices

Symbiont diversity may help coral reefs survive moderate climate change

Baskett ML, Gaines SD, Nisbet RM

A Further model derivation

In this supplement, we provide two model explorations: (1) a full derivation of the symbiont genetic model and (2) an analysis that explains the structure of the density dependence in the symbiont population model.

A.1 Genetic model derivation

First, we derive the symbiont genetic dynamics in eqn. (1)-(3) based on Lynch et al. (1991) (see also Lynch and Lande, 1993; Lynch, 1996). In particular, we derive the dynamics of the tolerance genotype (g) probability distribution $p_{im}(g)$ for each symbiont i in coral m as well as the symbiont population growth rate r_{im} in eq. (3). First, let $r_f^*(f, t)$ be the asymptotic growth rate of an individual with thermal tolerance phenotype f at time t . In addition, let the phenotype f given a genotype g be a random normal variable with mean g and environmental variance σ_e^2 , i.e., the phenotype probability distribution given genotype g is

$$q(f, g) = \frac{1}{\sqrt{2\pi\sigma_e^2}} e^{-\frac{(f-g)^2}{2\sigma_e^2}}. \quad (\text{A.1})$$

Therefore, the asymptotic growth rate of an individual with genotype g is

$$r_g^*(g, t) = \int r_f^*(f, t) q(f, g) df, \quad (\text{A.2})$$

and the total asymptotic population growth rate is

$$r_{im}(t) = \int r_g^*(g, t) p_{im}(g, t) dg. \quad (\text{A.3})$$

In addition, define $F(C_m, \mathbf{S}_m)$ as the density-dependent component of eq. (1),

$$F(C_m, \mathbf{S}_m) = \frac{\hat{r}(t) \sum_j S_{jm}}{K_{Sm} C_m}, \quad (\text{A.4})$$

where the vector $\mathbf{S}_m = (S_{1m}, S_{2m})$. Then the realized growth rate given genotype g is $r_g(g, t) = r_g^*(g, t) - F(C_m, \mathbf{S}_m)$, and the realized growth rate of the entire population is $\bar{r}_{im} = r_{im} - F(C_m, \mathbf{S}_m)$, where $\frac{dS_{im}}{dt} = \bar{r}_{im} S_{im}$ (Lande and Shannon, 1996). Given the above definitions, the dynamics of the thermal tolerance genotype probability distribution are

$$\frac{dp_{im}}{dt} = p_{im}(g, t)(r_g^*(g, t) - r_{im}(t)) \quad (\text{A.5})$$

(fig. 1a; Lynch et al., 1991). Note that the functional form of density dependence we use leads to genotype distribution dynamics unaffected by density dependence.

To define the phenotype-dependent instantaneous growth rate $r_f^*(f, t)$, for mathematical tractability we use stabilizing selection given an optimal phenotype and selection strength. The phenotype f is the temperature for which an individual is adapted, and the optimal phenotype $\theta(t)$ is the actual temperature. Let σ_{wm} determine the width of the fitness function, i.e., increasing σ_{wm} means decreasing selection strength. In addition, the maximum possible population growth rate \hat{r}_{im} depends on temperature such that it follows the empirically-determined relationship of increasing exponentially with the actual temperature $\theta(t)$ given constants a and b , or $\hat{r} = ae^{b\theta(t)}$ (Norberg, 2004). Given these parameters, the asymptotic growth rate for a phenotype f is

$$r_f^*(f, t) = \left(1 - \frac{(f - \theta(t))^2}{2\sigma_{wm}^2}\right) ae^{b\theta(t)} \quad (\text{A.6})$$

(Lynch et al., 1991; Norberg, 2004).

We assume that the genotypic distribution $p_{im}(g, t)$ is a normal distribution with mean \bar{g}_{im} and variance σ_{gim}^2 . Then substituting eq. (A.6) into eqs. (A.2)-(A.3) yields the asymptotic growth rate for a population with the genotypic distribution $p_{im}(g, t)$ in eq. (3) (Lynch et al., 1991). In addition, the genotypic distribution dynamics in eq. (A.5) and the asymptotic growth rate function in eq. (A.6) yield the dynamics of the mean genotype dynamics ($\int g \frac{dp_{im}(g,t)}{dt} dg$) in eq. (1) and (given the rate at which mutation increases the genetic variance σ_M^2) the genetic variance dynamics ($\frac{d}{dt}[\int (g - \bar{g}_{im})^2 p_{im}(g, t) dg]$) in eq. (2) (Lynch et al., 1991). Although constant genetic variance is often a simplifying assumption in quantitative genetic models, accounting for changes in genetic variance can be important to the dynamics of models with strong selection (Barton, 1999) and coevolution (Kopp and Gavrilets, 2006). Note that the constant rate at which mutation increases the genetic variance used here limits the potential rate of evolution but does not limit the absolute amount of evolution possible.

A.2 Symbiont density-dependence

Second, we analyze the symbiont competitive dynamics to explain the model structure with symbiont density dependence scaled by the maximum growth rate \hat{r} (rather than the realized population growth rate r_{im}). For this analysis, we use a simplified version of the model that ignores symbiont evolutionary dynamics ($\frac{d\bar{g}_{im}}{dt} = \frac{d\sigma_{gim}}{dt} = 0$) and temperature fluctuations in time (constant θ and therefore symbiont average and maximum population growth rates r_{im} and \hat{r}) in order to allow tractable equilibrium analysis. Furthermore, to use the simplest possible model that incorporates symbiont competition, we focus on one coral species (C) and ignore coral dynamics under the assumption that coral dynamics are much slower than symbiont dynamics such that coral cover is relatively constant on the time scale of symbiont competitive dynamics. Therefore, we follow two symbiont types with the dynamics

$$\frac{dS_1}{dt} = \frac{S_1}{K_S C} (r_1 K_S C - \hat{r}(S_1 + S_2)) \quad (\text{A.7})$$

$$\frac{dS_2}{dt} = \frac{S_2}{K_S C} (r_2 K_S C - \hat{r}(S_1 + S_2)), \quad (\text{A.8})$$

where all of parameters are the same as in the main text (note that, for these parameters, we lose the m subscripts because we do not need to differentiate between multiple coral species).

We analyze eqn. (A.7)-(A.8) by determining the local stability of each biologically relevant (i.e., non-negative) equilibrium based on the leading eigenvalue of the Jacobian matrix evaluated at that equilibrium. From this analysis, we find:

- The zero equilibrium ($\bar{S}_1 = \bar{S}_2 = 0$) is locally stable if both symbionts have negative realized population growth rates ($r_1, r_2 < 0$) and locally unstable if at least one symbiont has a positive realized population growth rate.
- Each edge equilibrium ($\bar{S}_1 = 0, \bar{S}_2 = K_S C r_2 / \hat{r}$ or $\bar{S}_2 = 0, \bar{S}_1 = K_S C r_1 / \hat{r}$) is locally stable if the symbiont type with a nonzero population size has the greater realized population growth rate ($r_1 < r_2$ or $r_2 < r_1$, respectively) and locally stable otherwise.
- The internal equilibrium ($\bar{S}_1, \bar{S}_2 > 0$) can only exist if the symbionts are genetically equivalent ($r_1 = r_2$), thus it is irrelevant to exploring competition between different symbiont types.

In summary, we find that if both symbionts have negative realized population growth rates ($r_1, r_2 < 0$), then the zero equilibrium ($\bar{S}_1 = \bar{S}_2 = 0$) is the only locally stable equilibrium, as we would expect intuitively. If at least one symbiont has a positive realized population growth rate, then the only locally stable equilibrium is the edge equilibrium for the symbiont with the greater realized population growth rate (i.e., if $r_2 < r_1$, the only locally stable equilibrium is $\bar{S}_1 = K_S C r_1 / \hat{r}$ and $\bar{S}_2 = 0$, and vice versa).

Therefore, assuming at least one symbiont has a positive realized population growth rate for the temperature at a given point in time, we expect the system to approach the equilibrium with only the symbiont type that has the greater realized population growth rate for that temperature. Thus, given the realized population growth rate in eq. (3), the symbiont with the thermal tolerance closest to the temperature is the competitive dominant. We employ this model structure in order to have the symbiont competitive outcome depend on the temperature without the use of additional parameters (e.g., temperature- or symbiont-type-dependent α_{ij} parameters and/or carrying capacities if we were to use a more traditional Lotka-Volterra competition model structure).

Note that the equilibrium symbiont density ($\bar{S}_i = K_S C r_i / \hat{r}$) is lower than the total carrying capacity ($K_S C$) unless the symbiont is optimally adapted to the temperature ($r_i = \hat{r}$). Therefore, the model structure allows for lower symbiont densities given low levels of thermal stress (temperatures deviating from the symbiont genotype such that $0 < r_i < \hat{r}$). If we had instead chosen to scale intraspecific density dependence by r_i rather than \hat{r} , then this intermediate outcome would not have been possible; rather, the model would result in an all-or-nothing equilibrium outcome of either zero symbiont density in a bleaching event ($r_i < 0, \bar{S}_i = 0$) or symbionts at their carrying capacity otherwise ($r_i > 0, \bar{S}_i = K_S C$). The temperature-dependent continuum of possible symbiont densities in our model structure (fig. A.1) better represents the biological reality (e.g., Fitt et al., 2000).

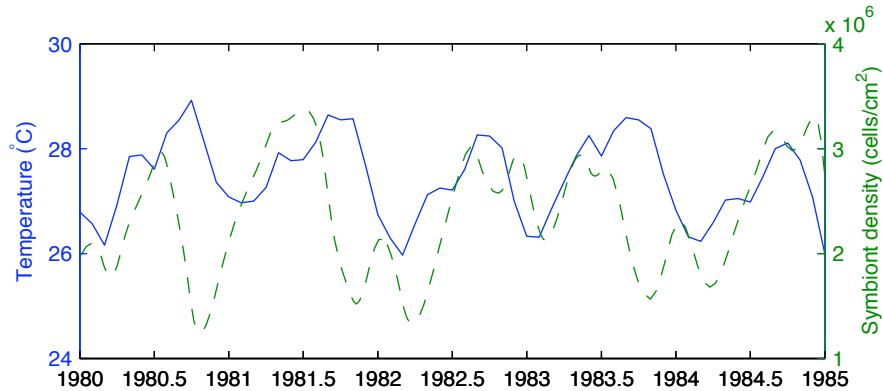


Figure A.1: Intra-annual fluctuations in symbiont density (green broken line) and temperature (blue solid line): five years from the simulation with one evolving symbiont and past (ISST) temperature data for Curaçao (excerpt from data presented in fig. 2).

References

- Barton, N. H. 1999. Clines in polygenic traits. *Genet. Res.*, **74**:223–236.
- Fitt, W. K., F. K. McFarland, M. E. Warner, and G. C. Chilcoat. 2000. Seasonal patterns of tissue biomass and densities of symbiotic dinoflagellates in reef corals and relation to coral bleaching. *Limnol. Oceanogr.*, **45**:677–685.
- Kopp, M. and S. Gavrillets. 2006. Multilocus genetics and the coevolution of quantitative traits. *Evolution*, **60**:1321–1336.
- Lande, R. and S. Shannon. 1996. The role of genetic variation in adaptation and population persistence in a changing environment. *Evolution*, **50**:434–437.
- Lynch, M. 1996. A quantitative-genetic perspective on conservation issues. In J. C. Avise and J. L. Hamrick, editors, *Conservation Genetics*, pages 471–501. Chapman and Hall, New York, NY.
- Lynch, M., W. Gabriel, and A. M. Wood. 1991. Adaptive and demographic responses of plankton populations to environmental-change. *Limnol. Oceanogr.*, **36**:1301–1312.
- Lynch, M. and R. Lande. 1993. Evolution and extinction in response to environmental change. In P. M. Kareiva, J. G. Kingsolver, and R. B. Huey, editors, *Biotic interactions and global change*, pages 234–250. Sinauer Associates Inc., Sunderland, Massachusetts.
- Norberg, J. 2004. Biodiversity and ecosystem functioning: A complex adaptive systems approach. *Limnol. Oceanogr.*, **49**:1269–1277.

B Symbiont distribution across a latitudinal gradient

In this supplement, we present model results exploring the dominant symbiont type along a latitudinal gradient of temperatures. Ulstrup et al. (2006) report different symbiont compositions at different latitudes in the Great Barrier Reef, with the potentially more thermally tolerant *Symbiodinium* D dominating northern locations and the potentially less tolerant *Symbiodinium* C dominating central and southern locations. Comparing model predictions to this latitudinal gradient tests how well our representation of symbiont community diversity (two symbiont types differing in 1°C in their optimal temperatures) represents clade-level symbiont diversity. For our model predictions, we simulated a one-coral (branching-type), two-symbiont model given the past temperature trajectories for the reefs sampled along this latitudinal gradient. When given initial mean genotypes of 26°C and 27°C, model predictions match this empirically observed trend, both without (fig. B.1) and with (fig. B.2) evolutionary dynamics.

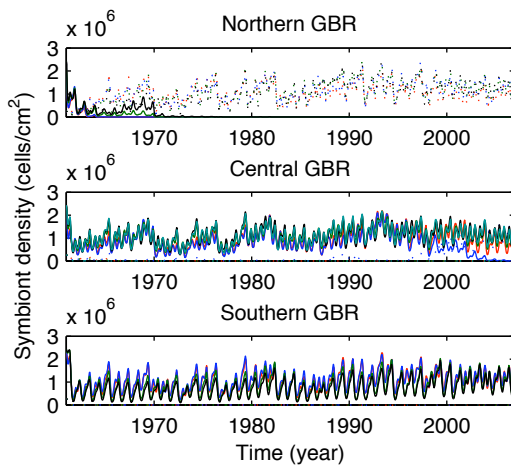


Figure B.1: Simulation predictions with one coral, two symbionts, and no evolution: symbiont density over time given past SST data (ISST) and multiple locations in the Great Barrier Reef (GBR regions across rows, with individual locations in different colors). The solid and dotted lines represent the less and more thermally tolerant type, respectively.

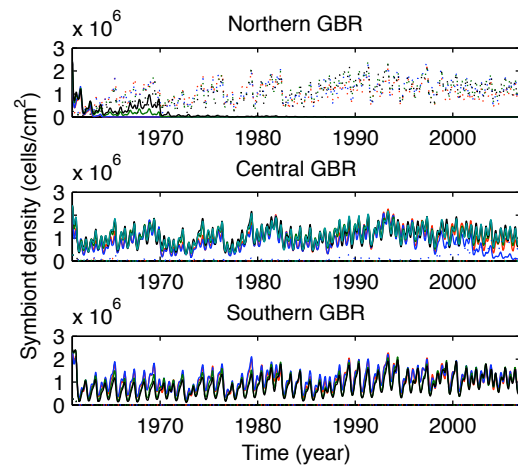


Figure B.2: Simulation predictions with one coral, two symbionts, and evolution: symbiont density over time given past SST data (ISST) and multiple locations in the Great Barrier Reef (GBR regions across rows, with individual locations in different colors). The solid and dotted lines represent the less and more thermally tolerant type, respectively.

References

Ulstrup, K. E., R. Berkelmans, P. J. Ralph, and M. J. H. van Oppen. 2006. Variation in bleaching sensitivity of two coral species across a latitudinal gradient on the Great Barrier Reef: the role of zooxanthellae. *Mar. Ecol. Prog. Ser.*, **314**:135–148.

C Test of model assumptions

We made many simplifying assumptions in the construction of the model presented here. In this supplement, we test the importance of two key simplifying assumptions: closed symbiont dynamics and complete coral phototrophy.

Experimental evidence suggests that, after bleaching events, previously unobserved symbionts may infect corals (Lewis and Coffroth, 2004), which we do not account for when assuming closed symbiont dynamics in the original model. To explore the impact of open symbiont dynamics on the model outcome, we replace eq. (1) with:

$$\frac{dS_{im}}{dt} = r_o C_m + \frac{S_{im}}{K_{S_m} C_m} \left(r_{im}(t) K_{S_m} C_m - \hat{r}(t) \sum_j S_{jm} \right), \quad (\text{C.1})$$

where r_o is the rate of symbiont infection from populations outside the coral, and all other terms are as before. Using $r_o = 5 \cdot 10^4 \text{ cells}\cdot\text{cm}^{-2}\cdot\text{yr}^{-1}$ based on Lewis and Coffroth (2004), we test the impact of open symbiont dynamics on model predictions with multiple symbiont types (and without evolution because the selection pressures on symbiont thermal tolerance outside the coral are unknown). Preliminary results indicate that open symbiont dynamics do not alter qualitative model trends under the parameter values used (fig. C.1).

Furthermore, corals may be able to obtain energy from sources outside symbionts, such as through heterotrophic feeding (Grottoli et al., 2006), which we ignore when assuming that coral growth and mortality depend directly on symbiont population sizes. To explore the impact of heterotrophic coral energy acquisition on the model outcome, we replace eq. (2) with:

$$\frac{dC_m}{dt} = C_m \left[\frac{\gamma_{hm} + \gamma_m \frac{\sum_i S_{im}}{K_{S_m} C_m}}{K_{C_m}} \left(K_{C_m} - \sum_n \alpha_{mn} C_n \right) - \frac{\mu_m}{1 + u_m \frac{\sum_i S_{im}}{K_{S_m} C_m}} \right], \quad (\text{C.2})$$

where γ_{hm} is the heterotrophic coral growth rate from energy gained independent of symbionts, and all other terms are as before. Using $\gamma_{hm} = 0.3814 \text{ yr}^{-1}$ assuming that the 21-35% percentage of the daily animal respiration from heterotrophy reported in Grottoli et al. (2006) resembles the percent contribution of heterotrophy to net coral growth when zooxanthellae are at carrying capacity, we test the impact of coral heterotrophy on model predictions. Preliminary results indicate that coral heterotrophy also does not alter qualitative model trends under the parameter values used (fig. C.2). However, note that these results assume constant coral heterotrophy; any potential for corals to up-regulate heterotrophy during bleaching events, as may occur for some species, may increase the potential for such corals to survive bleaching events and future climate change (Grottoli et al., 2006).

References

- Grottoli, A. G., L. J. Rodrigues, and J. E. Palardy. 2006. Heterotrophic plasticity and resilience in bleached corals. *Nature*, **440**:1186–1189.
- Lewis, C. L. and M. A. Coffroth. 2004. The acquisition of exogenous algal symbionts by an octocoral after bleaching. *Science*, **304**:1490–1492.

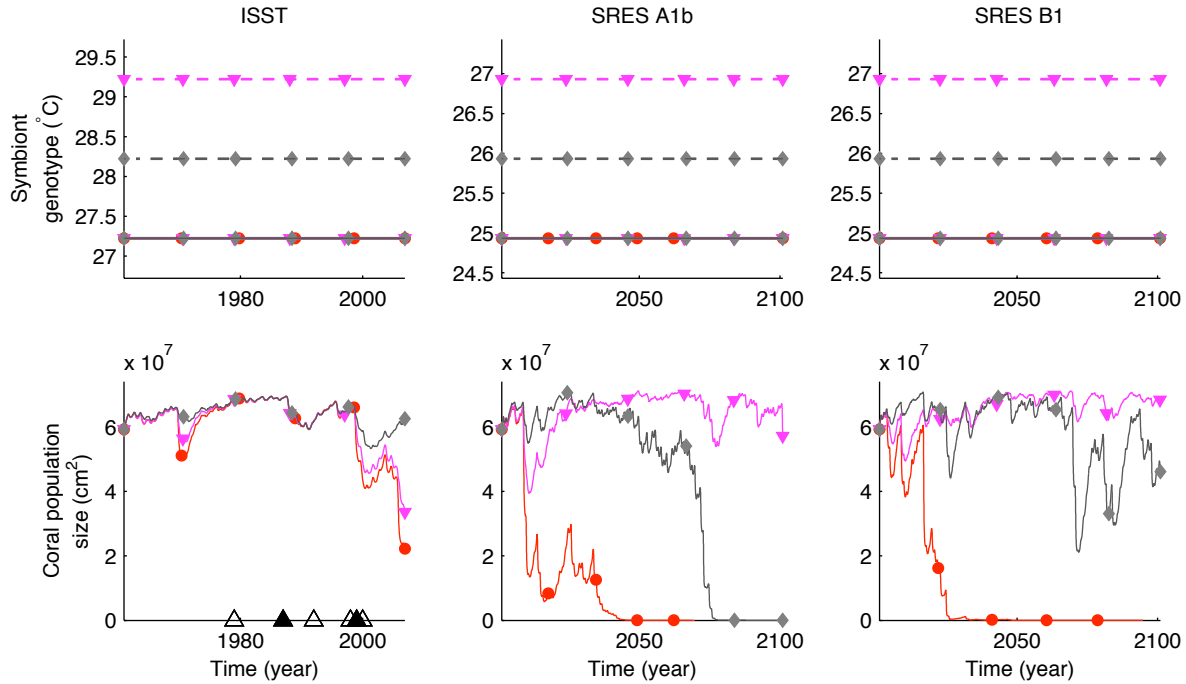


Figure C.1: Simulation predictions with one thermal-stress-susceptible, slow-growing coral and open symbiont dynamics. ISST is the past temperature data; SRES A1b and SRES B1 are the future temperature data with greater or less greenhouse gas emissions, respectively. Simulations with one symbiont are in red with circles, with two symbionts with a 1°C difference in thermal tolerance in gray with diamonds (solid lines for the first symbiont dynamics and broken lines for the second, more thermally tolerant symbiont dynamics), and with two symbionts with a 2°C difference in thermal tolerance in magenta with down-facing triangles; no simulations include evolution. In the coral population size plot with past temperature (ISST) data, filled and open up-facing triangles indicate observed major and minor bleaching events, respectively (Noordeloos et al., 2007). For comparison to closed symbiont dynamics, see lines with the same colors and symbols in figs. 2-3.

Noordeloos, M., M. Tupper, Y. Yusuf, M. Tan, S. Tan, S. Teoh, and S. Iqbal. 2007. ReefBase: A global information system on coral reefs. Online. Available from: <http://www.reefbase.org>.

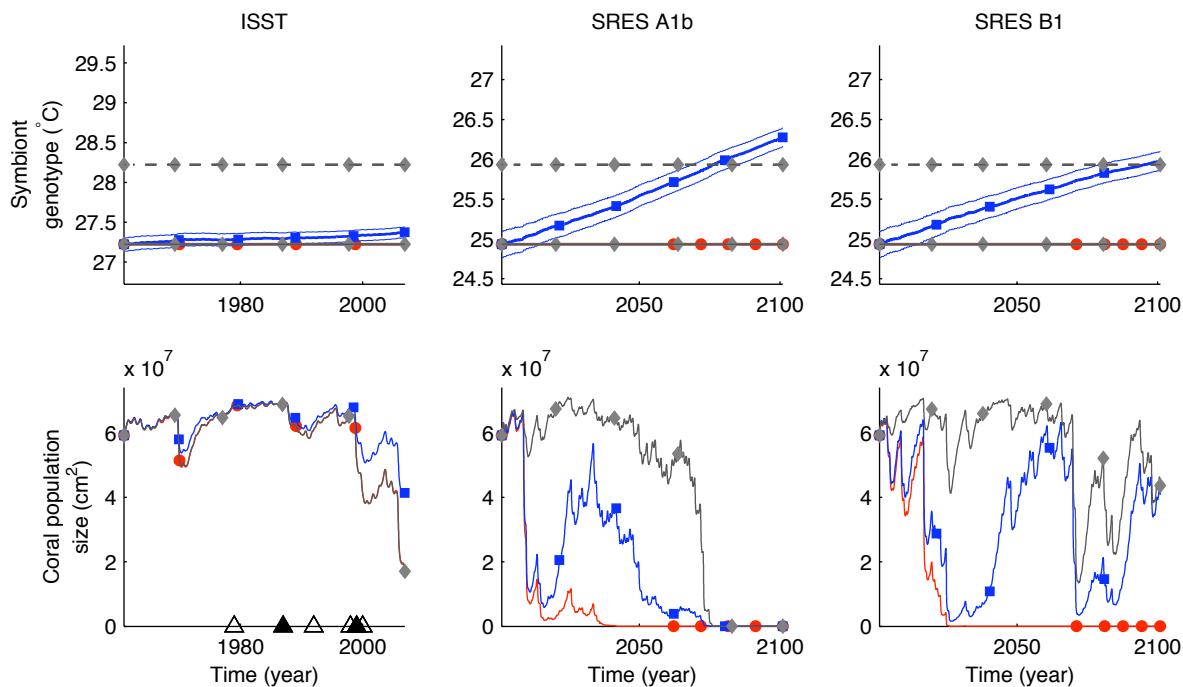


Figure C.2: Simulation predictions with one thermal-stress-susceptible, slow-growing coral and coral heterotrophy. ISST is the past temperature data; SRES A1b and SRES B1 are the future temperature data with greater or less greenhouse gas emissions, respectively. Simulations with one non-evolving symbiont are in red (circles). Simulations with one evolving symbiont are in blue (squares); genetic distribution 95% confidence intervals are shown in the genotype plots. Simulations with two non-evolving symbiont types are in gray (diamonds); solid and broken lines indicate the less and more thermally tolerant symbiont, respectively. For comparison to closed symbiont dynamics, see lines with the same colors and symbols in fig. 2.